Perfect Equalization for DMT Systems Without Guard Interval

Steffen Trautmann and Norbert J. Fliege, *Fellow, IEEE*

***Abstract*—We propose a new, low-complexity frequency-domain equalizer for discrete multitone (DMT) systems, which, in the absence of a guard interval, utilizes existing redundancy in the frequency domain to completely eliminate intersymbol and interchannel interferences. A perfect reconstruction condition is derived for the noise-free case leading to a sparse equalizer matrix structure. It is furthermore shown that under realistic scenarios minimum mean square error adaptation of the equalizer coefficients allows for nearly perfect reconstruction already for a much smaller amount of redundancy than indicated by the perfect reconstruction condition.**

The new equalization scheme has at least the same potential compared with traditional DMT while offering new degrees of freedom for designing short-latency DMT systems.

***Index Terms*—Bandwidth efficiency, discrete multitone, equalization, FEQ, intersymbol interference/interchannel interference, latency.**

I. Introduction

ONE OF THE main advantages of discrete multitone (DMT) systems is their simple receiver structure utilizing a channel equalizer with only one complex multiplication per carrier. This is achieved by introducing a time domain guard interval (GI) enabling the receiver to separate the steady-state response from the transient response of the transmission channel. The GI, placed between the symbols, has to be at least as long as the channel impulse response (CIR) in order to avoid intersymbol interference (ISI) and interchannel interference (ICI). This, however, severely restricts the achievable bandwidth efficiency especially for short-latency systems. Therefore, despite superior noise robustness, wider range and less power consumption, DMT was not adopted for HDSL2 systems [1].

To relax this problem, most DMT receivers apply an finite-impulse response (FIR) time domain equalizer (TEQ) before discrete Fourier transform (DFT) transform in order to shorten the effective length of the CIR (e.g., [2], [3]) . Further improvement can be achieved by shifting the TEQ to the frequency domain [4]. However, for complete equalization of the channel it is still necessary to add some kind of redundancy. Beside the common GI insertion, some authors aim to add redundancy by precoding techniques [5], while other utilize redundancy due to oversampling [6].

Alternatively, usage of frequency domain redundancy has been investigated as well. For most DMT implementations not every possible carrier is suited for data transmission. Hybrids in the signal path, finite transition of antialiasing and interpolation filters, and frequency-selective zeros in the channel spectrum limit the usable bandwidth. This generates a certain redundancy in the frequency domain, which may also be utilized for equalization. In [7], taking unused carriers into account for equalization was successfully applied to wavelet-based multitone (DWMT) systems with symbol-overlapping multiple-input–multiple-output (MIMO) receivers. Such a receiver structure can also be combined with a DMT transmitter, as we have shown in [8].

By exploitation of all structural degrees of freedom MIMO receivers offer maximum performance, but also require a high computational complexity for practical implementation. The receiver complexity can be reduced by splitting the MIMO structure into back transform to the frequency domain followed by a general linear combiner (LC) or frequency-domain equalizer (FEQ). Then, assuming a stronger impact on ISI/ICI from direct neighbors, the number of linear combinations can be limited to a small set of neighboring carriers and symbols. This reduction works well for DWMT systems with superior spectral selectivity of the transform basis filters [9], [10]. However, in the critically sampled case of DMT, without a GI and with every possible carrier used, any simplification of the FEQ structure significantly increases ISI/ICI. As a consequence, all approaches in the frequency domain for DMT systems have provided only moderate results so far.

In this paper, we present a new approach for the compensation of ISI and ICI distortions which is based on a surprising discovery: while linear combinations of output samples from arbitrary "normal used" carriers provide only poor compensation effects, samples from unused carriers have a strong impact on the equalization. With only a few linear combinations of unused carrier output samples perfect reconstruction can be achieved, i.e., ISI and ICI can totally be eliminated even in receiver structures without a GI. It turns out that the performance of the new equalization scheme is totally independent from the channel frequency response at the positions of the unused carriers. Thus, extra redundancy from normally unusable carriers can be utilized for ISI/ICI equalization without reducing the bandwidth efficiency, or increasing system latency. This is an essential advantage compared with the time domain GI solution. Furthermore, simulation results will show that optimal performance

Manuscript received March 30, 2001; revised December 14, 2001.

S. Trautmann was with the Mannheim University, Mannheim, Germany. He is now with the Telecommunications Research Center Vienna (ftw.), A-1220 Vienna, Austria (e-mail: trautmann@ftw.at).

N. J. Fliege is with the Mannheim University, D-68131 Mannheim, Germany (e-mail: fliege@informatik.uni-mannheim.de).

Publisher Item Identifier S 0733-8716(02)05368-4.

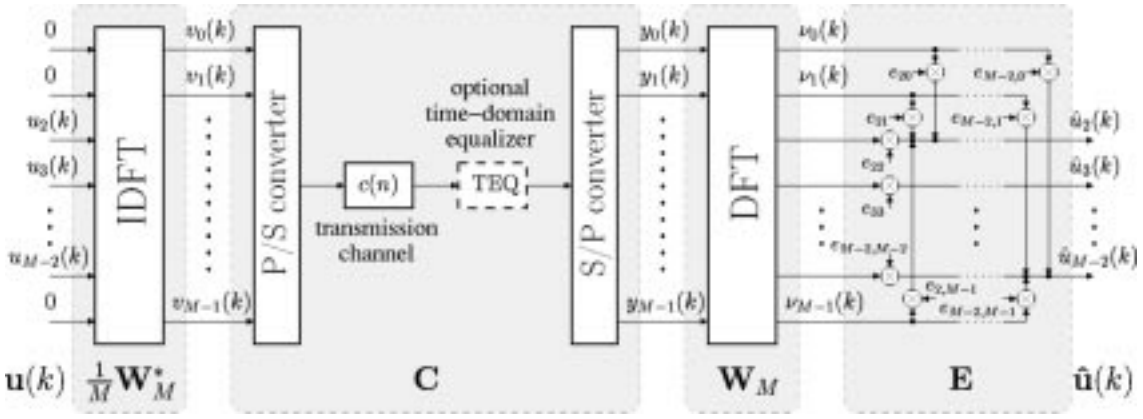

Fig. 1. DMT structure without GI, applying the new equalizer scheme (carriers 0, 1, and $M-1$ are not used for transmission).

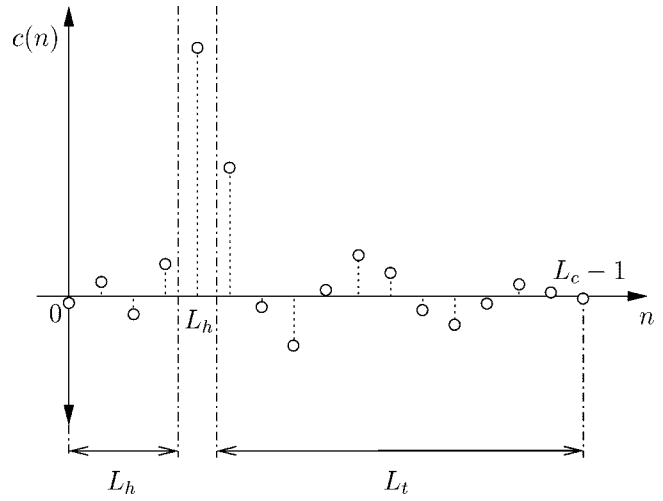

Fig. 2. Decomposition of the CIR into head part, peak coefficient, and tail part.

under realistic, noisy environments is already achieved with a very small number of unused carriers.

In the following context, we refer to our proposed method as "FEQ–DMT."

II. Perfect-Reconstruction (PR) Property

Consider a GI-less DMT system with transmitter DMT symbols $\mathbf{u}(k)$ consisting of M QAM-modulated elements $u_0(k)\dots u_{M-1}(k)$ and with receiver DMT symbols $\hat{\mathbf{u}}(k)$ as shown in Fig. 1. The discrete time-invariant transmission channel $c(n)=[c_0\ c_1\ \cdots\ c_{L_c-1}]$, afflicted with a propagation delay as illustrated in Fig. 2, contains the peak coefficient at discrete time instant $n=L_h$, enclosed by a preceding head part of L_h coefficients and a following tail part, consisting of L_t coefficients.

Assuming the length of the CIR as $L_c=L_h+L_t+1\le M$ with $L_t, L_h>0$, we have to deal with ISI/ICI from the preceding and the following DMT symbol. In order to describe these effects, we form a transmitter triple $\mathbf{u}^{(3)}(k)$ which is a series of three consecutive transmitted DMT symbols. Then, we define a transfer matrix $\mathbf{T}$ as $\hat{\mathbf{u}}(k)=\mathbf{T}\cdot\mathbf{u}^{(3)}(k)$ which in the ideal case without additive noise fulfills

$$\mathbf{T}=\mathbf{E}\cdot\underbrace{\mathbf{W}_M\cdot\mathbf{C}\cdot(\mathbf{I}_3\otimes\mathbf{W}_M^*/M)}_{\boldsymbol{\mathcal{H}}}\stackrel{!}{=}[\,\mathbf{0}_M\quad\mathbf{I}_M\quad\mathbf{0}_M\,]. \tag{1}$$

$\mathbf{E}$ represents the equalizer, while $\mathbf{W}_M$ and $\mathbf{W}_M^*/M$ specify the DFT and IDFT matrix, respectively, of size M. $\otimes$ symbolizes the Kronecker product, and $*$ defines transpose-conjugate operation. The Toeplitz-like channel matrix $\mathbf{C}$ describes the linear convolution of the IDFT-transformed transmitter triples with the CIR.

With the pseudoinverse $\boldsymbol{\mathcal{H}}^\dagger$ of $\boldsymbol{\mathcal{H}}$, defined as $\boldsymbol{\mathcal{H}}^\dagger=(\boldsymbol{\mathcal{H}}^*\boldsymbol{\mathcal{H}})^{-1}\boldsymbol{\mathcal{H}}^*$, we can calculate the equalizer matrix

$$\mathbf{E}=[\,\mathbf{0}_M\quad\mathbf{I}_M\quad\mathbf{0}_M\,]\cdot\boldsymbol{\mathcal{H}}^\dagger, \tag{2}$$

which allows for perfect reconstruction in a noise-free environment in case that $\boldsymbol{\mathcal{H}}\cdot\boldsymbol{\mathcal{H}}^\dagger=\mathbf{I}_M$. However, usually $\boldsymbol{\mathcal{H}}$ is not invertible, and we are unable to eliminate ISI/ICI from the neighboring symbols and carriers. Therefore, we have to investigate special nontrivial system structures different from GI insertion which provide a solution for (1).

In a first essential step, we figure out, which part of $\mathbf{C}$ allows for perfect reconstruction when using a common DMT receiver, and which part actually causes the interference we are trying to eliminate. As shown in Fig. 3, following the decomposition of $c(n)$ in Fig. 2, we can split $\mathbf{C}$ into three $M\times M$ blocks: a center part $\mathbf{C}_c$, a head part $\mathbf{C}_h$, and a tail part $\mathbf{C}_t$:

$$\mathbf{C}=[\,\mathbf{C}_t\quad\mathbf{C}_c\quad\mathbf{C}_h\,] \tag{3}$$

with

$$\mathbf{C}_t=\begin{bmatrix}0&\cdots&0&c_{L_c-1}&\cdots&c_{L_h+1}\\ \vdots&&&\ddots&\ddots&\vdots\\ \vdots&&&&\ddots&c_{L_c-1}\\ \vdots&&&&&0\\ \vdots&&&&&\vdots\\ 0&\cdots&\cdots&\cdots&\cdots&0\end{bmatrix} \tag{4}$$

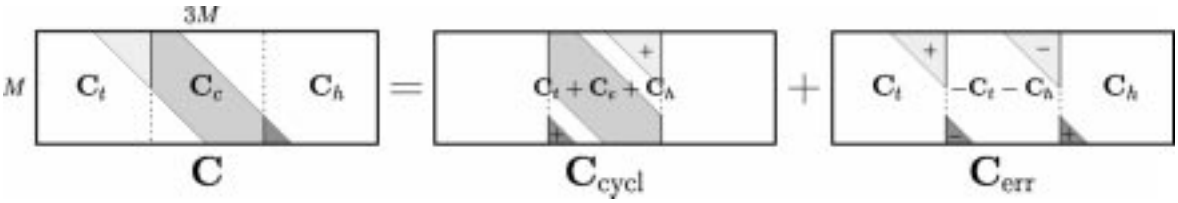

Fig. 3. Decomposition of the channel matrix into cyclic and error part.

$$\mathbf{C}_c = \begin{bmatrix} c_{L_h} & \cdots & c_0 & 0 & \cdots & 0 \\ \vdots & & & \ddots & \ddots & \vdots \\ c_{L_c-1} & & & & \ddots & 0 \\ 0 & \ddots & & & & c_0 \\ \vdots & \ddots & \ddots & & & \vdots \\ 0 & \cdots & 0 & c_{L_c-1} & \cdots & c_{L_h} \end{bmatrix} \tag{5}$$

and

$$\mathbf{C}_h = \begin{bmatrix} 0 & \cdots & \cdots & \cdots & \cdots & 0 \\ \vdots & & & & & \vdots \\ 0 & & & & & \vdots \\ c_0 & \ddots & & & & \vdots \\ \vdots & \ddots & \ddots & & & \vdots \\ c_{L_h-1} & \cdots & c_0 & 0 & \cdots & 0 \end{bmatrix}. \tag{6}$$

$\mathbf{C}_t \neq \mathbf{0}$ causes ISI from the preceding symbol, while $\mathbf{C}_h \neq \mathbf{0}$ generates ISI from the following symbol. Furthermore, because $\mathbf{C}_c$ does not possess a cyclic Toeplitz structure, ICI is introduced as well. Therefore, the ideal channel matrix—let us call it $\mathbf{C}_{\text{cycl}}$—would have $\mathbf{C}_t, \mathbf{C}_h = \mathbf{0}$ and the center block completed to a cyclic Toeplitz matrix. Thus, the remaining part $\mathbf{C} - \mathbf{C}_{\text{cycl}}$ must be responsible for ISI/ICI. As illustrated in Fig. 3, we obtain

$$\mathbf{C} = \underbrace{[\mathbf{0}_M \quad (\mathbf{C}_t + \mathbf{C}_c + \mathbf{C}_h) \quad \mathbf{0}_M]}_{\mathbf{C}_{\text{cycl}}} + \underbrace{[\mathbf{C}_t \quad (-\mathbf{C}_t - \mathbf{C}_h) \quad \mathbf{C}_h]}_{\mathbf{C}_{\text{err}}}. \tag{7}$$

Applying (7) to (1) leads to

$$\begin{aligned} &\mathbf{E} \cdot \mathbf{W}_M \cdot (\mathbf{C}_{\text{cycl}} + \mathbf{C}_{\text{err}}) \cdot (\mathbf{I}_3 \otimes \mathbf{W}_M^*/M) \\ &\quad = \mathbf{E} \cdot (\underbrace{\mathbf{W}_M \mathbf{C}_{\text{cycl}} (\mathbf{I}_3 \otimes \mathbf{W}_M^*/M)}_{\boldsymbol{\mathcal{H}}_{\text{cycl}}} \\ &\qquad + \underbrace{\mathbf{W}_M \mathbf{C}_{\text{err}} (\mathbf{I}_3 \otimes \mathbf{W}_M^*/M)}_{\boldsymbol{\mathcal{H}}_{\text{err}}}) \\ &\quad = [\mathbf{0}_M \quad \mathbf{I}_M \quad \mathbf{0}_M]. \end{aligned} \tag{8}$$

Now, after dividing $\boldsymbol{\mathcal{H}}$ into an ideal part and an error part, we can formulate two separate problems from (1)

$$\text{I.} \quad \mathbf{E} \cdot \boldsymbol{\mathcal{H}}_{\text{cycl}} \stackrel{!}{=} [\mathbf{0}_M \quad \mathbf{I}_M \quad \mathbf{0}_M] \tag{9}$$

and

$$\text{II.} \quad \mathbf{E} \cdot \boldsymbol{\mathcal{H}}_{\text{err}} \stackrel{!}{=} \mathbf{0}_{M \times 3M}. \tag{10}$$

First, $\mathbf{E}$ has to perfectly equalize the transmission over the cyclic channel part $\boldsymbol{\mathcal{H}}_{\text{cycl}}$. And second, with $\mathbf{E}$ the influence of the ISI/ICI part $\boldsymbol{\mathcal{H}}_{\text{err}}$ has to be completely eliminated as well.

With $\mathbf{C}_{\text{cycl, red}} = \mathbf{C}_t + \mathbf{C}_c + \mathbf{C}_h$, the cyclic part of the transfer matrix $\boldsymbol{\mathcal{H}}_{\text{cycl}}$ in (9) can be further simplified to

$$\boldsymbol{\mathcal{H}}_{\text{cycl}} = \mathbf{W}_M \cdot [\mathbf{0}_M \quad \mathbf{C}_{\text{cycl, red}} \mathbf{W}_M^*/M \quad \mathbf{0}_M]. \tag{11}$$

It can be shown that by singular value decomposition the cyclic Toeplitz matrix $\mathbf{C}_{\text{cycl, red}}$ equals to $\mathbf{C}_{\text{cycl, red}} = 1/M \cdot \mathbf{W}_M^* \cdot \mathbf{D} \cdot \mathbf{W}_M$ with the diagonal matrix $\mathbf{D} = \text{diag}(d_0, d_1, \ldots, d_{M-1})$ and $d_i = C(e^{j2\pi i/M})$ being the coefficients of the channel frequency response. Hence, the cyclic part is reduced to $\boldsymbol{\mathcal{H}}_{\text{cycl}} = [\mathbf{0}_M \quad \mathbf{D} \quad \mathbf{0}_M]$, and after elimination of the zero columns (9) can be rewritten as

$$\mathbf{E} \cdot \mathbf{D} = \mathbf{I}_M \tag{12}$$

with the obvious solution $\mathbf{E} = \mathbf{D}^{-1} = \text{diag}(e_0, e_1, \ldots, e_{M-1})$ and $e_i = 1/C(e^{j2\pi i/M})$. Note that this corresponds to the usual DMT one-tap-equalizer compensating the steady-state response of the transmission channel.

Realizing an equalizer according to (12), we have left no freedoms for solving (10). Only for the trivial constellation $\boldsymbol{\mathcal{H}}_{\text{err}} = \mathbf{0}$ a ISI/ICI-free transmission would be possible.

Returning to the initial situation, there exists at least one solution for (1) if the number of columns of matrix $\mathbf{E}$, i.e., the total number of carriers M, is equal to or larger than the number of linearly independent columns in $\boldsymbol{\mathcal{H}}$. One way to match this constellation is to assume that a certain number of carriers K is not used for transmission. Provided that no signal energy is distributed to unused carriers, with every additional unused carrier, three more columns in $\boldsymbol{\mathcal{H}}$ are multiplied by zero, i.e., are no longer relevant for solvability of (1). For a first moment one could think that we need to reduce the number of used carriers $N = M - K$ down to $N \leq M/3$ in order to fulfill the above condition. But we will see in the following context that this is only valid for the worst case.

Note that with K unused carriers the number of relevant rows in $\mathbf{E}$ is also reduced to N for equalization of the remaining used carriers.

For matrix notation of the mentioned elimination of nonrelevant rows and columns, we need to define a small set of selection matrices $\{\mathbf{S}_0, \mathbf{S}_1\}$ with

$$\mathbf{S}_1 = \text{diag}(s_0, s_1, \ldots, s_{M-1}) \tag{13}$$

with

$$s_i = \begin{cases} 1 & \text{if carrier is used} \\ 0 & \text{if carrier is not used} \end{cases}$$

and

$$\mathbf{S}_0 = \mathbf{I}_M - \mathbf{S}_1. \tag{14}$$

Shrinked to the nonzero columns, $\mathbf{S}_0$ is reduced to a $M \times K$ matrix $\mathbf{S}_{0,\,\mathrm{red}}$, and $\mathbf{S}_1$ to an $M \times N$ matrix $\mathbf{S}_{1,\,\mathrm{red}}$.

From the DFT output $\boldsymbol{\nu}(k)$, $\mathbf{S}_{1,\,\mathrm{red}}$ selects the samples of the used carriers, whereas $\mathbf{S}_{0,\,\mathrm{red}}$ collects the unused carrier DFT samples. Therewith, we can split $\mathbf{E}$ into two independent groups of equalizer coefficients

$$\mathbf{E} = \mathbf{E} \cdot \underbrace{(\mathbf{S}_0 + \mathbf{S}_1)}_{\mathbf{I}_M} = \underbrace{\mathbf{E} \cdot \mathbf{S}_0}_{\mathbf{E}_0} + \underbrace{\mathbf{E} \cdot \mathbf{S}_1}_{\mathbf{E}_1}. \tag{15}$$

where $\mathbf{E}_0$ contains all linear combinations with unused carrier output samples, and $\mathbf{E}_1$ includes the linear combinations with the used carrier output samples. Furthermore, with (15) we are able to distinguish between the free parameters in $\mathbf{E}$ in terms of solving either (9), or (10). Decomposition of $\mathbf{E}$ is depicted in Fig. 4 as well as derivation of the compact notations for $\mathbf{E}_0$ and $\mathbf{E}_1$ for better understanding of the following equations.

After cancellation of the zero columns and rows using $\mathbf{S}_{0,\,\mathrm{red}}$ and $\mathbf{S}_{1,\,\mathrm{red}}$ and substitution of (15), we write for (12)

$$\begin{aligned} &\mathbf{S}_{1,\,\mathrm{red}}^T \cdot (\mathbf{E}_0 + \mathbf{E}_1) \cdot \mathbf{D} \cdot \mathbf{S}_{1,\,\mathrm{red}} \\ &\quad = \mathbf{S}_{1,\,\mathrm{red}}^T \cdot (\mathbf{E} \cdot \underbrace{\mathbf{S}_0 \cdot \mathbf{D} \cdot \mathbf{S}_{1,\,\mathrm{red}}}_{=\mathbf{0}} + \mathbf{E}_1 \cdot \mathbf{D} \cdot \mathbf{S}_{1,\,\mathrm{red}}) \\ &\quad = \underbrace{\mathbf{S}_{1,\,\mathrm{red}}^T \cdot \mathbf{E}_1 \cdot \mathbf{S}_{1,\,\mathrm{red}}}_{\mathbf{E}_{1,\,\mathrm{red}}} \cdot \underbrace{\mathbf{S}_{1,\,\mathrm{red}}^T \cdot \mathbf{D} \cdot \mathbf{S}_{1,\,\mathrm{red}}}_{\mathbf{D}_{1,\,\mathrm{red}}} = \mathbf{I}_N. \end{aligned} \tag{16}$$

Solvability of this system is guaranteed. Completed to the full equalizer submatrix we obtain

$$\mathbf{E}_1 = \mathbf{S}_{1,\,\mathrm{red}} \cdot \mathbf{D}_{1,\,\mathrm{red}}^{-1} \cdot \mathbf{S}_{1,\,\mathrm{red}}^T. \tag{17}$$

Note that $\mathbf{D}_{1,\,\mathrm{red}}$ represents a submatrix of $\mathbf{D}$. Therefore, $\mathbf{E}_1$ contains an incomplete diagonal matrix with the inverse channel coefficients at the used carrier frequencies. As desired, the solution of (9) is independent from $\mathbf{E}_0$. Hence, the free parameters in $\mathbf{E}_0$ may be completely used for solving (10).

Eliminating the nonrelevant rows and columns in (10) leads to

$$\mathbf{S}_{1,\,\mathrm{red}}^T \cdot \mathbf{E} \cdot \mathbf{W}_M \cdot \mathbf{C}_{\mathrm{err}} \cdot (\mathbf{I}_3 \otimes \mathbf{W}_M^* \mathbf{S}_{1,\,\mathrm{red}}) = \mathbf{0}_{N \times 3N}. \tag{18}$$

Following the definition of $\mathbf{S}_0$ and $\mathbf{S}_1$, in order to reduce $\mathbf{C}_{\mathrm{err}}$ to the nonzero parts, we need to construct additional selection matrices $\{\mathbf{Z}_c,\, \mathbf{S}_c\}$ with the corresponding reduced $(L_c - 1) \times M$ matrix $\mathbf{Z}_{c,\,\mathrm{red}}$ and $3M \times 2(L_c - 1)$ matrix $\mathbf{S}_{c,\,\mathrm{red}}$, respectively. Then, if we define $\mathbf{C}_{th} = [\,\mathbf{C}_t \quad -\mathbf{C}_h\,]$ and $\mathbf{C}_{th,\,\mathrm{red}}$ as the compact notation without zero columns and rows, the reduced matrix of the error part of the channel is

$$\begin{aligned} \underset{(L_c-1)\times 2(L_c-1)}{\mathbf{C}_{\mathrm{err,\,red}}} &= \mathbf{Z}_{c,\,\mathrm{red}} \cdot \mathbf{C}_{\mathrm{err}} \cdot \mathbf{S}_{c,\,\mathrm{red}} \\ &= [\,\mathbf{C}_{\mathrm{th,\,red}} \quad -\mathbf{C}_{\mathrm{th,\,red}}\,] \\ &= \mathbf{C}_{\mathrm{th,\,red}} \cdot [\,\mathbf{I}_{L_c-1} \quad -\mathbf{I}_{L_c-1}\,]. \end{aligned} \tag{19}$$

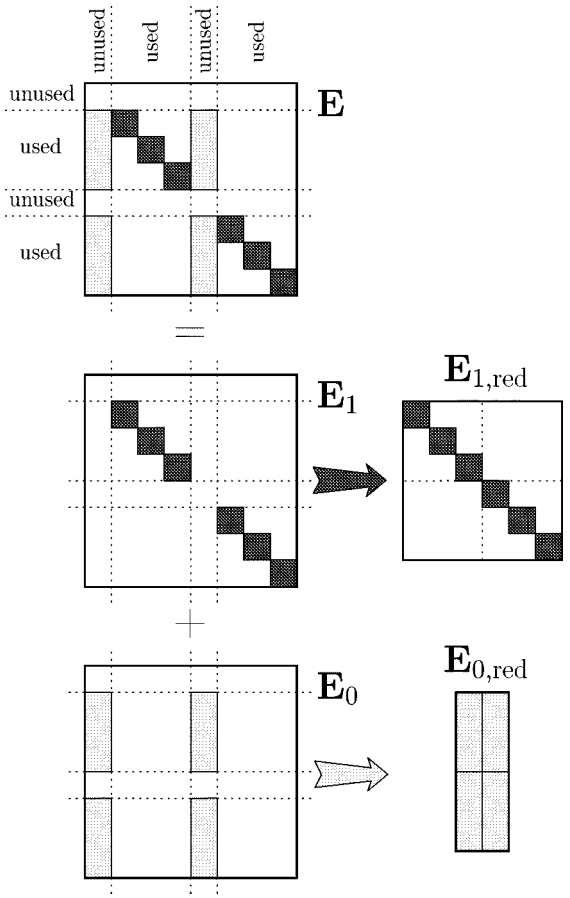

Fig. 4. Decomposition of the equalizer matrix and derivation of compact notation.

Substituting (15) and (19) in (18) and moving the $\mathbf{E}_{1,\,\mathrm{red}}$-dependent part to the right hand side, it follows:

$$\begin{aligned} &\underbrace{\mathbf{S}_{1,\,\mathrm{red}}^T \mathbf{E}_0 \mathbf{S}_{0,\,\mathrm{red}}}_{\mathbf{E}_{0,\,\mathrm{red}}} \cdot \underbrace{\mathbf{S}_{0,\,\mathrm{red}}^T \mathbf{W}_M \mathbf{Z}_{c,\,\mathrm{red}}^T}_{\mathbf{W}_{0,\,\mathrm{red}}} \cdot \mathbf{C}_{\mathrm{th,\,red}} \\ &\qquad \cdot \underbrace{[\,\mathbf{I} \quad -\mathbf{I}]\mathbf{S}_{c,\,\mathrm{red}}^T (\mathbf{I}_3 \otimes \mathbf{W}_M^* \mathbf{S}_{1,\,\mathrm{red}})}_{\boldsymbol{\mathcal{W}}_{\mathrm{red}}^*} \\ &\quad = -\underbrace{\mathbf{S}_{1,\,\mathrm{red}}^T \mathbf{E}_1 \mathbf{S}_{1,\,\mathrm{red}}}_{\mathbf{E}_{1,\,\mathrm{red}}} \cdot \underbrace{\mathbf{S}_{1,\,\mathrm{red}}^T \mathbf{W}_M \mathbf{Z}_{c,\,\mathrm{red}}^T}_{\mathbf{W}_{1,\,\mathrm{red}}} \cdot \mathbf{C}_{\mathrm{th,\,red}} \\ &\qquad \cdot [\,\mathbf{I} \quad -\mathbf{I}]\mathbf{S}_{c,\,\mathrm{red}}^T (\mathbf{I}_3 \otimes \mathbf{W}_M^* \mathbf{S}_{1,\,\mathrm{red}}) \end{aligned} \tag{20}$$

or in compact notation

$$\begin{aligned} \underset{N\times K}{\mathbf{E}_{0,\,\mathrm{red}}} \cdot \overbrace{\underset{K\times(L_c-1)}{\mathbf{W}_{0,\,\mathrm{red}}} \cdot \underset{(L_c-1)\times(L_c-1)}{\mathbf{C}_{\mathrm{th,\,red}}} \cdot \underset{(L_c-1)\times 3N}{\boldsymbol{\mathcal{W}}_{\mathrm{red}}^*}}^{\boldsymbol{\mathcal{H}}_{0,\,\mathrm{red}}} \\ = -\underset{N\times N}{\mathbf{E}_{1,\,\mathrm{red}}} \cdot \underset{N\times(L_c-1)}{\mathbf{W}_{1,\,\mathrm{red}}} \cdot \mathbf{C}_{\mathrm{th,\,red}} \cdot \boldsymbol{\mathcal{W}}_{\mathrm{red}}^*. \end{aligned} \tag{21}$$

This system is only solvable if the number of linearly independent columns in $\boldsymbol{\mathcal{H}}_{0,\,\mathrm{red}}$ is not greater than the number of free parameters K. It is known that the number of independent columns of a matrix product equals the minimum number of independent columns within all factors. While $\mathbf{W}_{0,\,\mathrm{red}}$ as a part of the DFT

matrix and $\mathbf{C}_{th,\,\mathrm{red}}$ for most realistic channels $c(n)$ can be assumed to have full column rank, it can be shown that $\boldsymbol{\mathcal{W}}^{*}_{\mathrm{red}}$ has a structure like

$$\boldsymbol{\mathcal{W}}^{*}_{\mathrm{red}} = \begin{bmatrix} \mathbf{A} & -\mathbf{A} & \mathbf{0}_{L_t \times N} \\ \mathbf{0}_{L_h \times N} & \mathbf{B} & -\mathbf{B} \end{bmatrix}. \tag{22}$$

A further explanation of $\mathbf{A}$ and $\mathbf{B}$ is not necessary. It is only important to recognize that $\boldsymbol{\mathcal{W}}^{*}_{\mathrm{red}}$ has only $2N$ independent columns. Therefore, (21) has at least one solution, if $K \geq \min(L_c - 1,\, 2N)$. This leads to two special cases.

Case 1

$\boldsymbol{K \geq L_c - 1, L_c - 1 < 2N}$: In this case, perfect equalization is always possible if the CIR is not longer than the number of unused carriers plus one.

Case 2

$\boldsymbol{K \geq 2N}$, $\boldsymbol{L_c - 1 \geq 2N}$: This is only the case if $N \leq M/3$. The maximum channel length for perfect equalization is then only restricted by the chosen model boundaries in (1). With $L_{h,\,\max} = M$ and $L_{t,\,\max} = M$ channels up to a length of $2M + 1$ coefficients fulfill this condition.

Note that for channels without propagation delay, i.e., $L_h = 0$, $\boldsymbol{\mathcal{W}}^{*}_{\mathrm{red}}$ is reduced to N independent columns, and already for $N \leq M/2$ used carriers we would be able to equalize channels up to a length of $M + 1$ coefficients.

From the practical point of view it is rather unlikely to use only a third of all possible carriers as required for case 2. We will, therefore, concentrate on the constellation described by case 1. Then, without limiting the number of solutions, all possible $\mathbf{E}_{0,\,\mathrm{red}}$ which solve (21) can also be found by solving the simplified system

$$\mathbf{E}_{0,\,\mathrm{red}} \cdot \mathbf{W}_{0,\,\mathrm{red}} = -\mathbf{E}_{1,\,\mathrm{red}} \cdot \mathbf{W}_{1,\,\mathrm{red}}. \tag{23}$$

Assuming the existence of the (pseudo)-inverse of $\mathbf{W}_{0,\,\mathrm{red}}$, which means that $K \geq L_c - 1$, and substituting (17), then $\mathbf{E}_0$ is calculated as follows:

$$\mathbf{E}_0 = -\mathbf{S}_{1,\,\mathrm{red}} \cdot \mathbf{D}^{-1}_{1,\,\mathrm{red}} \cdot \mathbf{W}_{1,\,\mathrm{red}} \cdot \mathbf{W}^{\dagger}_{0,\,\mathrm{red}} \cdot \mathbf{S}^{T}_{0,\,\mathrm{red}}. \tag{24}$$

Summarizing the results of this section, we obtain a dependence between CIR length and necessary number of unused carriers which is equivalent to the relation between CIR length and GI length for common DMT: Starting with $L_c = 1$ and $K = 0$ for the trivial solution without redundancy, with every additional unused carrier, the CIR length is allowed to be one coefficient longer for perfect equalization.

Note that perfect equalization only makes sense in a virtually noise-free environment. Thus, the condition $K \geq L_c - 1$ represents the worst case, i.e., the maximum need of redundancy. For an additive white Gaussian noise (AWGN)-afflicted channel, the number of unused carriers actually needed for optimal minimum mean-square-error (MMSE) performance is much smaller, as will be shown in Section IV.

Interestingly, (17) and (24) only depend on the channel frequency response at the used carrier frequencies in $\mathbf{D}_{1,\,\mathrm{red}}$. Transmission characteristics of the unused carriers is of no importance, because only the ISI/ICI leakage into these carriers is utilized for equalization. Here, the supposed disadvantage of the DFT basis filters becomes a clear advantage. Due to its worse spectral selectivity, ISI/ICI energy is spread almost uniformly to all carriers, not only to the nearest neighbors. In other words, carriers which are normally unsuitable for data transmission, suddenly receive a complete new importance. We do not need to sacrifice the "good" carriers in flat areas of the frequency response for optimal FEQ performance. When introducing redundancy in the frequency domain, it is sufficient to choose the K worst carriers in terms of attenuation.

III. Noise Robustness

In this section, we will show that for a certain number of unused carrier constellations, noise enhancement of the zero-forcing (ZF) solution can be kept constant for all carriers and limited to a reasonable level. Alternatively, an MMSE-based optimization of the equalizer coefficients is also presented, which takes additive noise into account and allows for arbitrary unused carrier arrangements.

A. Noise Sensitivity of the ZF Solution

Computation of the equalizer coefficients after a ZF constraint as presented in Section II allows for optimal results if no or very little additive noise is present. It is, however, commonly known that ZF equalizers tend to noise amplification, and performance decreases as soon as additive channel noise reaches a certain value. For our proposed method, noise amplification of the ZF solution is strongly dependent on the positions of unused carriers utilized for equalization. Thus, it may be possible to find a few constellations where noise enhancement is small enough for practical implementation. In the following we will show that indeed for a limited number of periodic unused-carrier arrangements the resulting noise after equalization remains white with a maximum amplification by 3 dB in relation to common DMT.

We remember that $\mathbf{E}_1$ as a part of $\mathbf{E}$ equals the one-tap-equalizer scheme used for DMT. Therefore, if we assume an AWGN-channel with uncorrelated noise on each carrier, and $\mathbf{E}_0 \neq \mathbf{0}$, a certain noise enhancement compared with DMT is inevitable. Furthermore, when inverting $\mathbf{W}_{0,\,\mathrm{red}}$, especially for large symbol lengths M, we obtain huge values in $\mathbf{W}^{\dagger}_{0,\,\mathrm{red}}$ which cause significant noise amplification in the equalized symbol.

If we define the noise amplification factor for carrier index i as the ratio $v_{n,\,i} = \mathbf{e}_i \mathbf{e}^{*}_i / \mathbf{e}_{1,\,i} \mathbf{e}^{*}_{1,\,i}$, where $\mathbf{e}_i$ and $\mathbf{e}_{1,\,i}$ specify the ith rows of $\mathbf{E}$ and $\mathbf{E}_1$, respectively, we obtain in logarithmic notation

$$\mathbf{v}_{n,\,\mathrm{dB}} = 10 \cdot \log_{10}(\mathbf{1}_{N \times 1} + \mathrm{diag}(\mathbf{W}_{1,\,\mathrm{red}} \mathbf{W}^{\dagger}_{0,\,\mathrm{red}} \cdot \mathbf{W}^{\dagger *}_{0,\,\mathrm{red}} \mathbf{W}^{*}_{1,\,\mathrm{red}})). \tag{25}$$

The vector $\mathbf{v}_{n,\,\mathrm{dB}}$ contains the noise amplification factors $v_{n,\,i,\,\mathrm{dB}}$ for each carrier, and $\mathbf{1}_{N \times 1}$ represents a column vector with N ones. The $\mathrm{diag}(\cdot)$ operator applied to a matrix extracts a column vector from the main diagonal of that matrix.

It turns out that the inner product $\mathbf{W}^{\dagger}_{0,\,\mathrm{red}} \cdot \mathbf{W}^{\dagger *}_{0,\,\mathrm{red}}$ tends to contain large coefficients depending on the unused carrier

arrangement. From the definition of the pseudo inverse, it would be desirable if between $\mathbf{W}_{0,\mathrm{red}}^{\dagger}$ and $\mathbf{W}_{0,\mathrm{red}}^{*}$ a relation like

$$\begin{aligned}\mathbf{W}_{0,\mathrm{red}}^{\dagger} &= \alpha \cdot \mathbf{W}_{0,\mathrm{red}}^{*} \\ (\mathbf{W}_{0,\mathrm{red}}^{*}\mathbf{W}_{0,\mathrm{red}})^{-1} \cdot \mathbf{W}_{0,\mathrm{red}}^{*} &= \alpha \cdot \mathbf{W}_{0,\mathrm{red}}^{*}\end{aligned} \tag{26}$$

could be established. This requires that $\mathbf{W}_{0,\mathrm{red}}^{*}\mathbf{W}_{0,\mathrm{red}}$ equals a scaled identity matrix, i.e., $\mathbf{W}_{0,\mathrm{red}}$ has to be a unitary matrix. If we replace $\mathbf{W}_{0,\mathrm{red}}$ with the submatrices from (20) it follows that:

$$\mathbf{Z}_{c,\mathrm{red}} \cdot \mathbf{W}_{M}^{*} \cdot \underbrace{\mathbf{S}_{0,\mathrm{red}}\mathbf{S}_{0,\mathrm{red}}^{T}}_{\mathbf{S}_0} \cdot \mathbf{W}_{M} \cdot \mathbf{Z}_{c,\mathrm{red}}^{T} = 1/\alpha \cdot \mathbf{I}_{L_c-1}. \tag{27}$$

The matrix $\mathbf{W}_{M}^{*}\mathbf{S}_0\mathbf{W}_{M}$ represents a cyclic Toeplitz matrix with the first row $[\mathbf{W}_{M} \cdot \mathbf{s}_0]^T$, where $\mathbf{s}_0 = \mathrm{diag}(\mathbf{S}_0)$ contains the main diagonal elements of the column selection matrix $\mathbf{S}_0$. $\mathbf{S}_0$ has K ones and N zeros in the diagonal. Thus, the diagonal elements of $\mathbf{W}_{M}^{*}\mathbf{S}_0\mathbf{W}_{M}$ are always constant and equal to K, i.e., $\alpha = 1/K$. But only for the (useless) special case that $\mathbf{S}_0 = \mathbf{I}_M$, $\mathbf{W}_{M}^{*}\mathbf{S}_0\mathbf{W}_{M}$ equals a diagonal matrix as desired. Therefore, the following reduction to the relevant rows and columns using $\mathbf{Z}_{c,\mathrm{red}} \cdot \cdots \cdot \mathbf{Z}_{c,\mathrm{red}}^{T}$ should lead us to a diagonal matrix. For any pair $\{L_h, L_t\}$ assuming a constant L_c, this is only possible if

$$\mathbf{W}_{M} \cdot \mathbf{s}_0 = [K \underbrace{0 \cdots 0}_{L_c-2} x \cdots x \underbrace{0 \cdots 0}_{L_c-2}]^T. \tag{28}$$

Given this formation, $\mathbf{W}_{0,\mathrm{red}}^{\dagger} \cdot \mathbf{W}_{0,\mathrm{red}}^{\dagger *}$ simplifies to $1/K \cdot \mathbf{I}$. Substituting this relation in (25) and considering that all diagonal elements in

$$\mathbf{W}_{1,\mathrm{red}}\mathbf{W}_{1,\mathrm{red}}^{*} = \mathbf{S}_{1,\mathrm{red}}^{T}\mathbf{W}_{M}\underbrace{\mathbf{Z}_{c,\mathrm{red}}^{T}\mathbf{Z}_{c,\mathrm{red}}}_{\mathbf{Z}_c}\mathbf{W}_{M}^{*}\mathbf{S}_{1,\mathrm{red}} \tag{29}$$

are equal to $L_c - 1$, we obtain a constant noise amplification for all carriers

$$v_{n,i,\mathrm{dB}} = v_{n,\mathrm{dB}} = 10 \cdot \log_{10}\left(1 + \frac{L_c - 1}{K}\right), \tag{30}$$

which can be at most 3 dB with respect to a DMT one-tap equalizer, provided that $K \geq L_c - 1$.

Since $s_{0,i} \in \{0, 1\}$ and accordingly $\mathbf{W}_{M}\mathbf{s}_0$ is conjugate symmetric, the number of possible $\mathbf{s}_0$ for a desired constellation corresponding to (28) is rather limited. For arbitrary $\mathbf{s}_0$, only in case that $L_c = 2$ considerable noise enhancement can be prevented. Only one unused carrier is sufficient under this condition. However, further redundancy reduces the noise amplification to $v_n = 10 \cdot \log_{10}(1 + 1/K)$.

Considering the special properties of the DFT, we know that the transformed vector $\mathbf{W}_{M}\mathbf{s}_0$ has an arrangement according to (28) if $\mathbf{s}_0$ shows a periodic pattern with an integer period $p = M/(L_c - 1)$. This helps us to derive a few special cases which are useful for practical implementation:

a) Baseband DMT Transmission (DMT-Based xDSL Like ADSL, VDSL) In case of real baseband transmission, independent from the transmission channel characteristics, carriers at $f = 0$ and $f = f_S/2$ cannot be used for complex modulation. Then, the main diagonal of $\mathbf{S}_0$ equals

$$\mathbf{s}_0 = [1 \underbrace{0 \cdots 0}_{M/2-1} 1 \underbrace{0 \cdots 0}_{M/2-1}]^T. \tag{31}$$

$\mathbf{s}_0$ shows a pattern with period $M/2$. Thus, the DFT results in

$$\mathbf{W}_{M} \cdot \mathbf{s}_0 = [2 \quad 0 \quad 2 \quad 0 \quad \cdots \quad 2 \quad 0]^T. \tag{32}$$

ISI/ICI can be eliminated for channels up to an effective length of three coefficients. Noise amplification is either 1.76 dB ($L_c = 2$) or 3 dB ($L_c = 3$). Any further unused carriers may be used to reduce the noise amplification.

b) Pilot-Based DMT Transmission For time-variant transmission channels, equidistant, so-called pilot carriers with a fixed content are used for permanent update of the channel estimate. We combine the pilot samples p_i within one DMT symbol to a pilot symbol $\mathbf{p} = [p_0 \quad p_1 \quad \cdots \quad p_{K-1}]^T$ and first define the fixed content of the pilots $\mathbf{p} = \mathbf{0}$, which of course only makes sense under insufficient orthogonality conditions, i.e., in the presence of ISI/ICI. With no transmission over these carriers, the available redundancy may be additionally used for equalization. It is only required to have a symbol length which is an integer multiple of the pilot distance. Then, we have

$$\mathbf{s}_0 = [1 \underbrace{0 \cdots 0}_{M/K-1} 1 \underbrace{0 \cdots 0}_{M/K-1} 1 \cdots 0]^T, \tag{33}$$

and accordingly

$$\mathbf{W}_{M} \cdot \mathbf{s}_0 = [K \underbrace{0 \cdots 0}_{K-1} K \underbrace{0 \cdots 0}_{K-1} K \cdots 0]^T. \tag{34}$$

A DMT system with K pilot carriers fulfilling the above conditions has the ability to ideally equalize channels up to a length of $K + 1$ coefficients without a GI. According to (30), and depending on the redundancy exploitation, additive noise is kept white and amplified to at most 3 dB.

Even if the pilots $\mathbf{p}$ are different from zero, perfect reconstruction is always possible. However, in this case, a column reduction of the equation system by right-hand side multiplication with $\mathbf{S}_{1,\mathrm{red}}$ as in (18) cannot be applied. Then, an additional condition to compensate the interference of the pilot symbol into the data symbol can be described by

$$\mathbf{S}_{1,\mathrm{red}}^{T} \cdot \mathbf{E} \cdot \boldsymbol{\mathcal{H}} \cdot (\mathbf{I}_3 \otimes \mathbf{S}_{0,\mathrm{red}}) = \mathbf{0}_{N \times 3K}. \tag{35}$$

By multiplying the known pilot symbol $\mathbf{p}$ we end up with one additional equation, or column, respectively, for subsystem II in (20)

$$\begin{aligned}&\mathbf{E}_{0,\mathrm{red}} \cdot \underbrace{(\mathbf{S}_{0,\mathrm{red}}^{T}\boldsymbol{\mathcal{H}}_{\mathrm{err}}(\mathbf{I}_3 \otimes \mathbf{S}_{0,\mathrm{red}})(\mathbf{1}_{3\times 1} \otimes \mathbf{p}) + \mathbf{S}_{0,\mathrm{red}}^{T}\mathbf{D}\mathbf{S}_{0,\mathrm{red}}\mathbf{p})}_{K \times 1} \\ &\quad = -\mathbf{E}_{1,\mathrm{red}} \cdot \underbrace{(\mathbf{S}_{1,\mathrm{red}}^{T}\boldsymbol{\mathcal{H}}_{\mathrm{err}}(\mathbf{I}_3 \otimes \mathbf{S}_{0,\mathrm{red}}))(\mathbf{1}_{3\times 1} \otimes \mathbf{p})}_{N \times 1}.\end{aligned} \tag{36}$$

Therefore, the maximum length of an equalizable CIR given K nonzero pilots reduces to K coefficients.

B. MMSE-Based Optimization

The restriction to periodic unused carrier arrangements usually does not allow us to utilize all existing redundancy in the frequency domain. Furthermore, computation after a perfect-reconstruction constraint is definitely not matched to realistic conditions. A MMSE-based optimization of the FEQ coefficients which minimizes the mean squared error $\mathcal{E}_{\mathrm{MSE}}$ between the delayed input symbol $\mathbf{u}(k-d)$ and the output symbol $\hat{\mathbf{u}}(k)$

$$\begin{aligned}\mathcal{E}_{\mathrm{MSE}} &= \frac{1}{M}\sum_{i=0}^{M-1} E\{|\hat{u}_i(k)-u_i(k-d)|^2\} \\ &= \frac{1}{M}\mathrm{trace}\{E\{(\mathbf{u}(k-d)-\hat{\mathbf{u}}(k)) \\ &\qquad \cdot(\mathbf{u}(k-d)-\hat{\mathbf{u}}(k))^*\}\} \end{aligned} \tag{37}$$

is more suitable for noise-afflicted channels.

If $\boldsymbol{\nu}(k)$ describes the DFT output, the reconstructed receive symbol $\hat{\mathbf{u}}_{\mathrm{red}}(k)$ without unused carrier samples follows from:

$$\hat{\mathbf{u}}_{\mathrm{red}}(k) = \underbrace{\mathbf{S}_{1,\,\mathrm{red}}^{T}\mathbf{E}}_{\mathbf{E}_{\mathrm{red}}}\cdot\boldsymbol{\nu}(k). \tag{38}$$

Then, with $\mathbf{e}_i$ as the ith row of $\mathbf{E}_{\mathrm{red}}$ and $\mathbf{R}_{\nu\nu}$ as the autocorrelation matrix of $\boldsymbol{\nu}(k)$ we obtain

$$\begin{aligned}\mathcal{E}_{\mathrm{MSE}} = \frac{1}{N}\sum_{i=0}^{N-1}[&\sigma_{u_i}^2 + \mathbf{e}_i\mathbf{R}_{\nu\nu}\mathbf{e}_i^* - \mathbf{e}_i E\{\boldsymbol{\nu}(k)u_i^*(k-d)\} \\ &- E\{u_i(k-d)\boldsymbol{\nu}^*(k)\}\mathbf{e}_i^*]. \end{aligned} \tag{39}$$

Comparing (38) with (1), considering additive noise $\mathbf{r}(k)$ on the transmission channel, and reducing $\boldsymbol{\nu}(k)$ and $\mathbf{u}(k)$ to the nonzero part leads to

$$\begin{aligned}\boldsymbol{\nu}_{\mathrm{red}}(k) = &\underbrace{\mathbf{Z}_{i,\,\mathrm{red}}\mathbf{W}_M\cdot\mathbf{C}_T}_{\mathbf{F}_{i,\,\mathrm{red}}} \\ &\cdot\left(\underbrace{\mathbf{C}_P\cdot(\mathbf{I}_3\otimes\mathbf{W}_M^*/M\cdot\mathbf{S}_{1,\,\mathrm{red}})}_{\boldsymbol{\mathcal{H}}_{\mathrm{red}}}\mathbf{u}_{\mathrm{red}}^{(3)}(k)+\mathbf{r}(k)\right). \end{aligned} \tag{40}$$

Here, $\mathbf{Z}_{i,\,\mathrm{red}}$ selects the nonzero elements in $\mathbf{e}_i$, whereas $\mathbf{S}_{1,\,\mathrm{red}}$ collects the N used carrier input samples from $\mathbf{u}(k)$. Accordingly, $\mathbf{u}_{\mathrm{red}}^{(3)}(k)$ represents three consecutive input symbols $\mathbf{u}_{\mathrm{red}}(k)$ in compact notation without unused carrier zeros. The channel matrix $\mathbf{C}$ is split into two submatrices $\mathbf{C}=\mathbf{C}_T\cdot\mathbf{C}_P$ in order to incorporate the effects of noise coloring due to the optional FIR-TEQ. $\mathbf{C}_P$ defines the physical channel, and $\mathbf{C}_T$ symbolizes the convolution with the TEQ. In case that no TEQ is used, we have $\mathbf{C}_P=\mathbf{C}$ and $\mathbf{C}_T=\mathbf{I}$.

Substituting (40) into (39) and assuming a zero-mean, white noise process $\mathbf{r}(k)$ with constant noise energy σ_r^2 in all carriers, the mean squared error results in

$$\begin{aligned}\mathcal{E}_{\mathrm{MSE}} = \frac{1}{N}\sum_{i=0}^{N-1}[&\mathbf{e}_{i,\,\mathrm{red}}\mathbf{F}_{i,\,\mathrm{red}}(\underbrace{\boldsymbol{\mathcal{H}}_{\mathrm{red}}\mathbf{R}_{uu}\boldsymbol{\mathcal{H}}_{\mathrm{red}}^*}_{\mathbf{R}_{hh}}+\sigma_r^2\mathbf{I})\mathbf{F}_{i,\mathrm{red}}^*\mathbf{e}_{i,\,\mathrm{red}}^* \\ &+\sigma_{u_i}^2(1-\mathbf{e}_{i,\,\mathrm{red}}\mathbf{F}_{i,\,\mathrm{red}}\mathbf{h}_{\mathrm{red},\,(d-1)N+i} \\ &-\mathbf{h}_{\mathrm{red},\,(d-1)N+i}^*\mathbf{F}_{i,\,\mathrm{red}}^*\mathbf{e}_{i,\,\mathrm{red}}^*)] \end{aligned} \tag{41}$$

where $\mathbf{R}_{uu}$ is the autocorrelation matrix of $\mathbf{u}_{\mathrm{red}}^{(3)}(k)$, and $\mathbf{h}_{\mathrm{red},\,(d-1)N+i}$ corresponds to the $((d-1)N+i)$th row of $\boldsymbol{\mathcal{H}}_{\mathrm{red}}$. Partial derivation of this equation after $\mathbf{e}_i$ gives the optimal equalizer coefficients as follows:

$$\begin{aligned}\mathbf{e}_{i,\,\mathrm{red}} = &\sigma_{u_i}^2\mathbf{h}_{\mathrm{red},\,((d-1)N+i)}^*\mathbf{F}_{i,\,\mathrm{red}}^* \\ &\cdot(\mathbf{F}_{i,\,\mathrm{red}}\mathbf{R}_{hh}\mathbf{F}_{i,\,\mathrm{red}}^*+\sigma_r^2\mathbf{F}_{i,\,\mathrm{red}}\mathbf{F}_{i,\,\mathrm{red}}^*)^{-1}. \end{aligned} \tag{42}$$

with $\mathbf{e}_i=\mathbf{e}_{i,\,\mathrm{red}}\mathbf{Z}_{i,\,\mathrm{red}}$.

As already mentioned it turns out that with MMSE adaptation of the FEQ coefficients nearly perfect equalization is already achieved with a much smaller number of unused carriers as expected from the PR condition. Clearly, FEQ–DMT is much less sensitive to a deviation from the PR condition compared with traditional DMT using a GI. While DMT introduces strong ISI/ICI as soon as the GI length is only a few taps shorter than the effective CIR length, FEQ–DMT appears to perform an indirect shortening of the CIR. This statement even holds true if the CIR length significantly overrides the DFT symbol length M. Thus, FEQ–DMT eliminates another restriction of the DMT algorithm, namely that the CIR has to fit within one DFT symbol in order to prevent time domain aliasing.

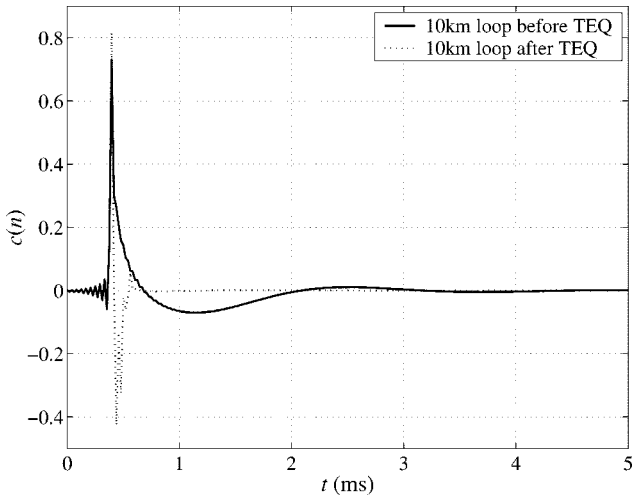

Fig. 5. (Normalized) CIR of a 10 km loop with 0.9 mm diameter, with and without TEQ.

IV. Simulation Results

Several design examples of the proposed FEQ scheme have been compared with original DMT modulation using a Matlab-simulated DMT system. The used channel characteristics were determined by an existing DMT system [11] on twisted-pair loops with lengths between 2 to 30 km and diameters of 0.8 or 0.9 mm. At a fixed sampling rate of $f_S = 48$ kHz, the impulse responses of the measured channels have a length of several hundred coefficients, shortened to approximately 9 to 13 coefficients using MMSE-optimized TEQ filters [12]. As an example, Figs. 5 and 6 show impulse and frequency response of a 10 km loop before and after TEQ shortening.

The simulation uses a sufficient number of random data symbols to estimate the noise component caused by ISI/ICI and AWGN.

We decided to consider data throughput for comparison in order to illustrate not only dependency on ISI/ICI errors, but also on bandwidth efficiency. Therefore, based on the estimated SNR a following Hughes–Hartogs adaptive loading algorithm [13]

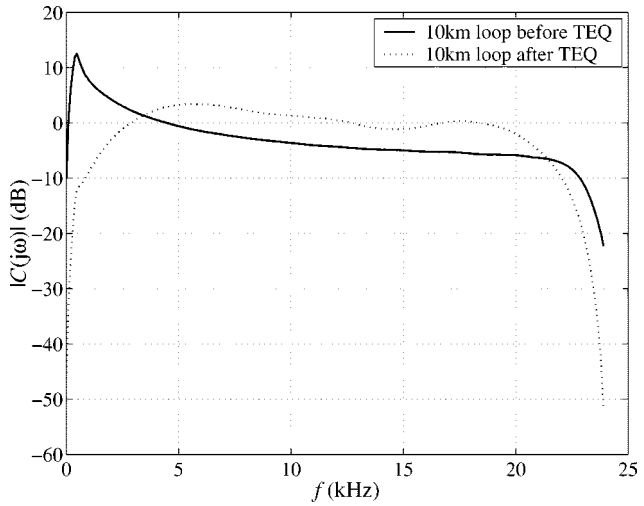

Fig. 6. (Normalized) channel frequency response of a 10 km loop with 0.9 mm diameter, with and without TEQ.

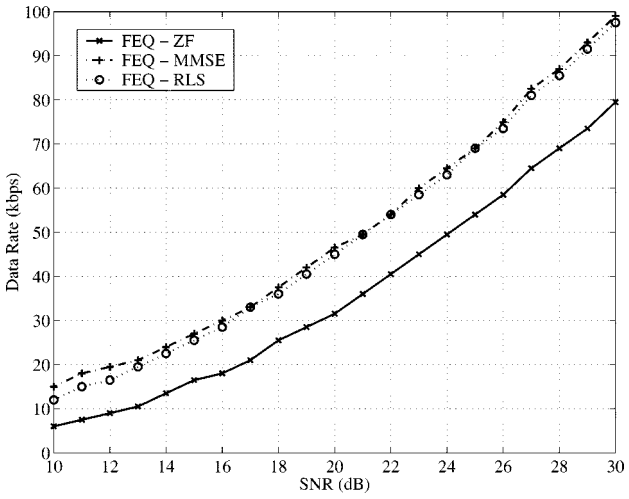

Fig. 8. Performance of FEQ–DMT for AWGN-distorted channel with different SNR (M =64, K =8).

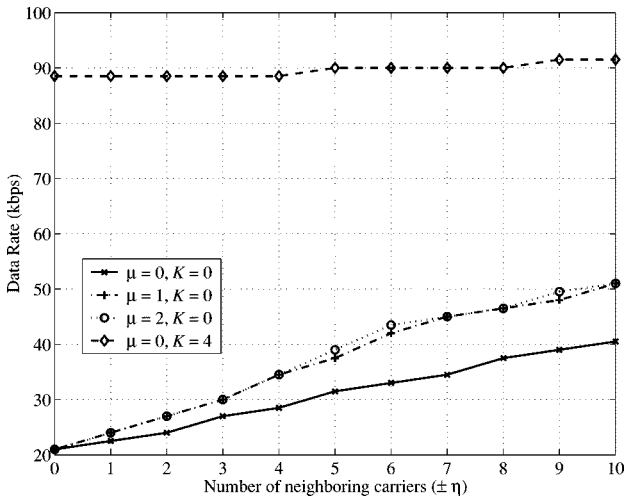

Fig. 7. FEQ performance of unused-carrier branch selection versus neighboring branch selection (M =64, SNR =30 dB).

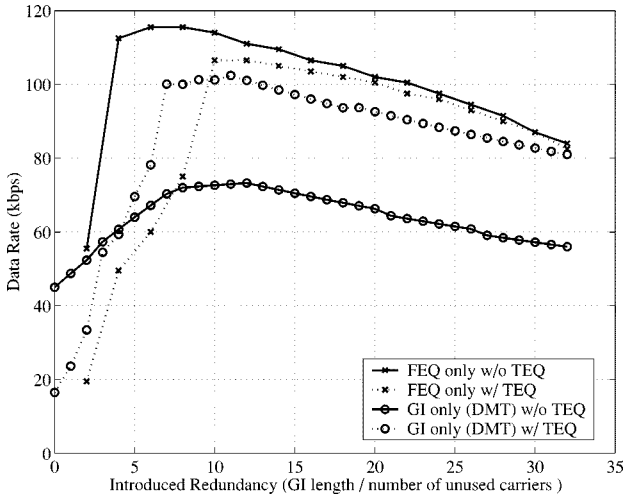

Fig. 9. Performance of FEQ–DMT versus DMT in dependence on TEQ usage (M =64, SNR =30 dB).

maximizes the data rate for constant sum transmission power and BER $= 10^{-8}$.

If not directly mentioned, we use a DFT length of $M = 64$, and a AWGN-distorted channel with SNR =30 dB. In general, we assume baseband transmission, i.e., for each DMT example, the carriers at DC and $f_S/2$ cannot be used.

Fig. 7 shows the data throughput for different reduced equalizer matrices $\mathbf{E}$. Symmetric constellations with η neighboring carriers and μ neighboring symbols to each side are considered for equalization. If $K > 0$ then unused carriers are also considered according to our proposed method. This leads to $((2\mu+1)(2\eta+1)+K)N$ active branches, or nonzero elements, respectively, in $\mathbf{E}$. Note that with $\mu > 0$ neighboring symbols are also considered for equalization, i.e., $\mathbf{E}$ becomes a rectangular $M \times (2\mu+1)M$ matrix, whereas FEQ–DMT only takes the present symbol into account. Without unused carriers performance is linearly increasing with the number of neighboring carriers. Taking the nearest neighboring symbols into account ($\mu = 1$) slightly increases the performance. Due to the effective length of the CIR, ISI is limited to the direct neighbored symbols, and $\mu > 1$ does not give any further improvement. Our proposed method with only four equidistant unused carriers and $\mu = \eta = 0$ clearly outperforms all other constellations with neighborhood branch selection at a much smaller complexity. Furthermore, if $K > 0$, any consideration of neighboring carriers does not give significant performance improvement. It is, therefore, sufficient to reduce $\mathbf{E}$ to the combination with unused carrier output samples.

As we can see in Fig. 8, ZF computation of the FEQ coefficients is most sensitive to noise. Alternatively, first numerical results using a common exponentially-weighted recursive-least-square (RLS) algorithm show robust and fast convergence close to the optimal MMSE solution. Usually, 50 to 100 iterations are sufficient for a weighting factor of $\gamma = 0.99$.

In order to demonstrate the CIR shortening capability of FEQ–DMT, Fig. 9 shows the performance of conventional DMT versus FEQ–DMT depending on the introduced redundancy either with, or without TEQ. MMSE optimization is applied for adaptation of the FEQ coefficients.

When using a TEQ we achieve optimum performance as expected for about K, $L_g = 10 \cdots 12$. Without TEQ the situation changes completely: While conventional DMT performance collapses due to severe ISI/ICI distortions, FEQ–DMT outperforms the TEQ-aided result with even less needed redundancy. We repeated this simulation for various twisted pair loops—each with more than 200 coefficients—with always the same observation: Typically, 8 to 12 unused carriers are sufficient for optimal FEQ performance. Although $L_c \gg K$, ISI/ICI distortion is kept below the level of typical background noise.

In contrary to the TEQ, FEQ–DMT allows for direct maximization of the data rate using simple linear methods for coefficient adaptation. Together with the gain in bandwidth efficiency by taking advantage of the two unusable carriers this explains the higher data rate of TEQ-less FEQ–DMT in comparison to original DMT with TEQ.

In general, the combination of FEQ–DMT with a separately adapted TEQ filter appears suboptimal if not obsolete at all.

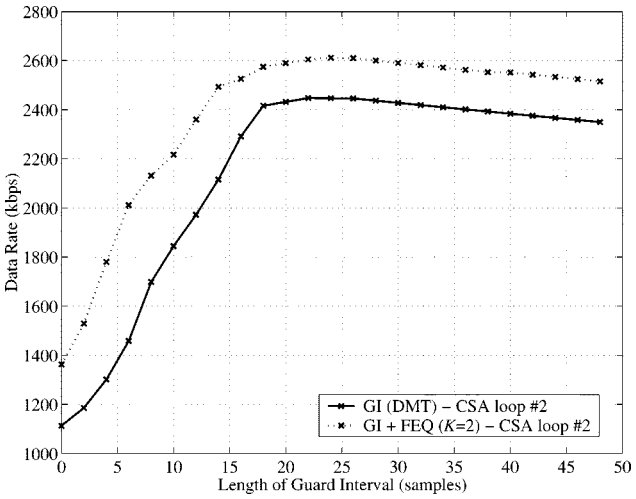

Fig. 10. Performance of baseband DMT with and without usage of frequency domain redundancy (M =512, f_S = 2.208 MHz, CSA loop #2, SNR =30 dB).

V. Conclusion and Outlook

With the proposed algorithm redundancy insertion of the DMT algorithm is completely shifted from the time domain to the frequency domain. Therewith, it becomes possible to utilize existing redundancy in the frequency domain, which normally remains unused when using traditional algorithms. For this purpose, the DMT single-tap equalizer is extended with additional branches from unused carrier DFT output samples. It was shown that, like traditional DMT, the new algorithm allows for perfect equalization of the receive signal under noise-free conditions.

One of the most interesting aspects which can be read from the perfect reconstruction condition is the fact that the channel characteristics at the position of the carriers used for the extended FEQ is of no importance. FEQ–DMT only utilizes the ISI/ICI leakage caused by the DFT operation at the receiver side. This leakage effect is especially strong and wide-spread for DMT "thanks" to the poor spectral selectivity of the DFT basis filters.

Over noisy channels, MMSE-adapted FEQ–DMT provides a much higher robustness against insufficient orthogonality conditions than conventional DMT. Without an additional TEQ it compensates for ISI/ICI and even time domain aliasing effects.

FEQ–DMT always provides the smallest possible latency time for a given parameter constellation, independent from the amount of introduced redundancy. This may not be very interesting for an ADSL scenario, where the GI has only 1/16th of the DFT symbol length. However, when designing DMT systems with significantly smaller latency compared with ADSL, optimal redundancy usage and minimum, redundancy-independent latency become essential preconditions.

In contrary to traditional CIR shortening using a TEQ, FEQ–DMT directly maximizes data throughput, separate for each carrier and with simple, well-investigated linear coefficient adaptation methods like LMS or RLS.

For typical values of K, complexity of the extended FEQ is similar if not smaller compared with a TEQ. That means when discarding the former obligatory TEQ, FEQ–DMT can be implemented without increasing the overall complexity.

In this paper, we have restricted the derivation of the new equalizer to the case where no GI is used. It is, however, possible to combine both, GI insertion and FEQ method. This allows for optimal distribution of redundancy, either to time or frequency domain, with respect to data rate, latency time, or complexity. Without explaining the mathematical background a first result is presented in Fig. 10. Different from the previous simulations, we used ADSL-conform DFT length, sampling rate, and bandwidth for this example in order to apply a standard test loop (CSA #2). An AWGN-distorted channel of SNR =30 dB was assumed. The solid line shows the data rate in dependence on the GI length for conventional DMT. The second line draws the performance of the same system, but now including the linear combination with only the two unusable carriers at DC and $f_S/2$. Especially for a small GI, performance is drastically increased while the complexity enhancement is almost negligible. Note that the effect of improving the bandwidth efficiency becomes even more significant with DFT lengths smaller than 512. Also, this example applies only two unused carriers for the extended FEQ. Each additional unused carrier would further improve the data throughput. Note also that we used a nine-tap TEQ filter in order to shorten the CIR of the CSA test loop. Without TEQ, performance of the conventional DMT system would be even worse compared with the combination of GI and FEQ.

Provided that unused carriers are available, the combination of GI and FEQ method allows to improve the performance of any kind of DMT receiver with no changes in the transmitter and without violating a standard. GI insertion in conjunction with the extended FEQ can be regarded as a generalization of the conventional DMT scheme and will be subject to further investigation.

References

[1] W. Goralski, *ADSL and DSL Technologies*. New York: McGraw-Hill, 1998.

[2] P. J. W. Melsa, R. C. Younce, and C. E. Rohrs, "Impulse response shortening for discrete multitone transceivers," *IEEE Trans. Commun.*, vol. 44, pp. 1662–1672, Dec. 1996.
[3] D. Pal, G. N. Iyengar, and J. M. Cioffi, "A new method of channel shortening with applications to discrete multi tone (DMT) systems," in *Proc. IEEE Int. Conf. Communications, ICC*, Atlanta, GA, June, 1998.
[4] K. Van Acker, G. Leus, M. Moonen, O. Van de Wiel, and T. Pollet, "Per tone equalization for DMT receivers," in *Proc. IEEE Global Telecommunications Conf., GLOBECOM*, Rio de Janeior, Dec., 1999.
[5] K.-W. Cheong and J. M. Cioffi, "Precoder for DMT with insufficient cyclic prefix," in *Proc. IEEE Int. Conf. Communications, ICC*, Atlanta, GA, June 1998.
[6] M. de Courville, P. Duhamel, P. Madec, and J. Palicot, "Blind equalization of OFDM systems based on the minimization of a quadratic criterion," in *Proc. IEEE Int. Conf. Communications, ICC*, Dallas, TX, June, 1996.
[7] S. Trautmann, T. Karp, and N. J. Fliege, "Using modulated filter banks for ISI/ICI-corrupted multicarrier transmission," in *Proc. SPIE Vol. 3813, Wavelet Applications in Signal and Image Processing VII*, Denver, CO, July 1999.
[8] S. Trautmann, T. Karp, and N. J. Fliege, "Comparing TEQ and MMSE receivers for short-latency DMT transmission," in *Proc. Int. OFDM Workshop*, Hamburg, 1999, pp. 20/1–20/4.
[9] S. D. Sandberg and M. A. Tzannes, "Overlapped discrete multitone modulation for high speed copper wire communications," *IEEE J. Select. Areas Commun.*, vol. 13, pp. 1571–1585, Dec. 1999.
[10] A. D. Rizos, J. G. Proakis, and T. Q. Nguyen, "Comparison of DFT and cosine-modulated filter banks in multicarrier modulation," in *Proc. GLOBECOM*, San Francisco, CA, Nov. 1994.
[11] S. Trautmann, G. Dickmann, and N. J. Fliege, "Realisierung eines 64-kBit-DMT-Modems für Zweidraht-Kupferleitungen bis 20 km Länge," in *Proc. OFDM-Fachgesprõch*, Braunschweig, Sept/ 1997.
[12] N. Al-Dhahir and J. M. Cioffi, "Optimum finite-length equalization for multicarrier transceivers," *IEEE Trans. Commun.*, vol. 44, pp. 56–64, Jan. 1996.
[13] D. Hughes and Hartogs, "Ensemble modem structure for imperfect transmission media," U.S. Patent 4 679 227 (July 1987), 4 731 816 (Mar. 1988) and 4 833 706 (May 1989).

Steffen Trautmann received the Dipl.-Ing. degree in Information Technology from the Dresden University of Technology, Dresden, Germany, in 1996. He was a Ph.D. student at the Hamburg University of Technology, Hamburg, Germany, from February 1996 to December 1996.

From October 1994 to April 1995, he was a Visiting Student at the University of Wisconsin, Madison. From 1997 to 2001, he was with the Mannheim University, Mannheim, Germany, as a Research and Teaching Assistant. After finishing his Ph.D. thesis, he is presently a Senior Researcher at the Telecommunications Research Center Vienna (ftw.), Vienna, Austria. His research interests include multirate signal processing, filter banks, equalization, interference suppression, channel and source coding and their application to telecommunications and image processing.

Norbert J. Fliege (M'89–SM'90–F'00) received the diplom degree (Dipl.-Ing.) and the doctor degree (Dr.-Ing.), in 1971, from the University of Karlsruhe, Germany.

Since 1978, he was an Associate Professor at the University of Karlsruhe. In 1980, he was a Visiting Professor at ESIEE in Paris. From 1982 to 1996, he was a Full Professor and Head of the Telecommunication Institute at Hamburg University of Technology in Hamburg, Germany. Since 1996, he has been a Full Professor of Electrical Engineering and Computer Technology at University of Mannheim, Germany. Since 1968, he has been engaged in research work on fields like active filters, digital filters, communication circuits and software, digital audio, and multirate digital signal processing. In addition, he served as a Department Chairman and as Head of a research center. He has also founded a company providing telecommunication equipment. He has published about 100 papers, most of them in international magazines and conference proceedings, and four books, one of them with the title *Multirate Digital Signal Processing* (New York: Wiley, 1994).

Dr. Fliege is a member of EURASIP, and a member of VDE (Germany). He has received several national and international awards. In 1997, he received the honorary doctorate from University of Rostock, Germany. In 2000, he was awarded an IEEE Fellow for contributions to analog and digital signal processing, and to engineering education.